

Resisting influence: How the strength of predispositions to resist control can change strategies for optimal opinion control in the voter model

Markus Brede^{1,2*}, Valerio Restocchi^{1,3} and Sebastian Stein¹

¹ Agents, Interactions, and Complexity group, ECS, University of Southampton, Southampton, UK

² Institute of Life Sciences, University of Southampton, Southampton, UK

³ Southampton Business School, University of Southampton, Southampton, UK

Correspondence*:

Markus Brede

brede.markus@gmail.com

2 ABSTRACT

In this paper we investigate influence maximization, or optimal opinion control, in a modified version of the two-state voter dynamics in which a native state and a controlled or influenced state are accounted for. We include agent predispositions to resist influence in the form of a probability q with which agents spontaneously switch back to the native state when in the controlled state. We argue that in contrast to the original voter model, optimal control in this setting depends on q : For low strength of predispositions q optimal control should focus on hub nodes, but for large q optimal control can be achieved by focusing on the lowest degree nodes. We investigate this transition between hub and low-degree node control for heterogeneous undirected networks and give analytical and numerical arguments for the existence of two control regimes.

Keywords: opinion control, voter dynamics, scale-free networks, optimization, influence maximization

1 INTRODUCTION

Processes of opinion formation play a role in a variety of real-world problems, ranging from political elections to marketing and product adoption, see (Castellano et al., 2009; Sirbu et al., 2016) for recent reviews. Very often these processes involve peer-to-peer interaction (Easley and Kleinberg, 2010) and thus take place on social networks. In this context the natural question arises how an external party with a certain amount of resources at its disposal can steer such a social system in a desired direction, maybe either with the intent of maximizing the adoption of products (Kempe et al., 2003; Bharathi et al., 2007, 2010; Goyal et al., 2014) or for the purposes of political influence in the so-called campaign problem (Hegselmann et al., 2015).

Starting with the seminal study of (Kempe et al., 2003) on influence maximization, work in this area has strongly focused on the independent cascade model or related versions of threshold models which have been studied in competitive and non-competitive settings (Kempe et al., 2003; Bharathi et al., 2007,

24 2010; Goyal et al., 2014). In the independent cascade model, influencing parties strategically distribute
25 seeds which can then cause cascades of influence spread. However, whilst allowing for neat solutions
26 using optimal percolation (Morone and Makse, 2015), in the independent cascade model agent behavior is
27 assumed to be fixed once committed to a certain opinion, thus not allowing for dynamical change subject
28 to competing internal or external influence over time. Models of this type thus appear not suitable for a
29 range of applications (Kuhlman et al., 2013) in which the interest is in dynamic opinion change.

30 Recognizing this limitation of the independent cascade model, recent work has also started to consider
31 opinion control in dynamic models of binary opinion change, which appear more suitable to capture
32 dynamic phenomena of opinion change if agents don't have strong commitment to decisions. Research
33 in this area so far has considered models based on the kinetic Ising model (Liu and Shakkottai, 2010;
34 Laciana and Rovere, 2011; Lynn and Lee, 2016), a variant of the AB model (Arendt and Blaha, 2015)
35 which results in majority-like dynamics, and the voter dynamics (Kuhlman et al., 2013; Yildiz et al., 2013;
36 Masuda, 2015). Whereas in the kinetic Ising model agents change opinions according to a majority-like
37 dynamics, in the voting dynamics agents adopt opinions of randomly selected neighbors (Clifford and
38 Sudbury, 1973; Holley and Liggett, 1975). In contrast to, e.g., the Glauber dynamics underlying the kinetic
39 Ising model, opinion changes of agents in the voting dynamics are caused by the pressure of the majority
40 of their neighbors only in an averaged sense and the state of the majority does not play a direct role when
41 making updating decisions. With differing effects of majority pressure one thus finds differences in model
42 behavior (Castellano et al., 2009). Nevertheless, of interest for our study below, for the kinetic Ising model,
43 recent work has pointed out that optimal influence allocations may shift from focusing at high-degree
44 nodes to low degree nodes depending on the *social* temperature of opinion change (Lynn and Lee, 2016).
45 The work of Lynn and Lee (2016) demonstrates that hub control may not be optimal for all types of social
46 contagion processes and hub nodes may play different roles at different stages of the dynamics (Quax
47 et al., 2013). However, the focus of the present study is on the voting dynamics. In this context, Mobilia
48 was first to investigate the impact of an agent favoring one opinion, a so-called 'zealot' (Mobilia, 2003;
49 Mobilia and Georgiev, 2005), which was later extended to considerations of inflexible voters (Mobilia et al.,
50 2007). Zealots, or partisan voters, can be interpreted as external influence on the system. Whereas in the
51 voting dynamics consensus is typically reached (Castellano et al., 2009), the mutual presence of multiple
52 opposing zealots can lead to the co-existence of different opinions in equilibrium (Mobilia and Georgiev,
53 2005; Mobilia et al., 2007). Effects of *zealotry* in the voting dynamics are of considerable interest in the
54 literature and have been studied in various settings. For instance, considerations of error-prone zealots have
55 been addressed in Masuda et al. (2010); Masuda and Redner (2011). Further recent studies include voter
56 models with a large number of states (Waagen et al., 2015), extensions to the non-linear q-voter model
57 (Mobilia, 2015), an exploration of the role of mass media in multi-state voter models (Hu and Zhu, 2017),
58 or, more recently, a study on the role of noise in the mean-field voter model with zealots (Khalil et al.,
59 2018). However, none of the latter studies consider the role of strategically placed zealots.

60 In the context of opinion control in the voter model Kuhlman et al. (2013) investigated control strategies
61 focused on the highest-degree nodes, attempting to minimize control costs to achieve given threshold
62 opinion shares. In other related work Yildiz et al. (2013) proposed a new algorithm to find optimal control
63 strategies, but mainly focused on the evaluation of the algorithm. Closest to the present work is the study
64 of Masuda (2015), in which methods from linear algebra are used to explore optimal opinion control in
65 the voter model. Masuda (2015) analyzes steady state solutions of the master equation and then carries
66 out numerical optimization to investigate optimal control strategies for artificially generated scale-free
67 Barabási-Albert networks (Albert and Barabási, 2002) and a range of empirical social networks, including
68 email-communication, co-authorship, and directed online social networks, finding that control protocols

69 that focus on the highest-degree nodes are generally successful in heterogeneous undirected networks, but
 70 not necessarily in the case of directed networks. Findings of previous work on opinion control in the voter
 71 model thus seem to generally agree that optimal control on undirected social networks should generally be
 72 focused but not exclusively be concentrated on high-degree nodes Kuhlman et al. (2013); Masuda (2015).
 73 However, whilst proposing new algorithms and proving analysis of optimal opinion control for certain
 74 network topologies, up to our best knowledge no previous study has investigated the role of the strength of
 75 predispositions to resist change on strategies for optimal opinion control.

76 Studies like (Masuda, 2015) have assumed the presence of two external influencing parties and
 77 investigated optimal strategies of an active optimizer competing against a passive strategy that does
 78 not actively pursue optimal control. Here we propose a slightly different variant of the voter model which
 79 may be closer in spirit to the independent cascade model but still allows for dynamic change of opinions.
 80 Instead of assuming the presence of a passive party, we consider a setting in which an active party attempts
 81 to align the system towards a goal, but agents are ‘fickle’ in the sense that they might also spontaneously
 82 revert to the uninfluenced state with some probability. The inclusion of such fickleness allows us to study
 83 the dependence of opinion control on the strength of predispositions of agents to resist change. As we shall
 84 argue below, optimal control strategies are indeed very different in low and high predisposition settings on
 85 undirected networks, pointing out that previous findings like those of Kuhlman et al. (2013) and Masuda
 86 (2015) might not apply in all settings.

87 With the inclusion of predispositions we aim to provide a framework that agrees with empirical evidence
 88 from recent work on social networks, in which it was observed that influence propagation follows a *complex*
 89 *contagion dynamics* (Centola and Macy, 2007; Centola et al., 2007; Hill et al., 2010; Centola, 2010; Romero
 90 et al., 2011). Complex contagion describes a process whereby repeated exposure is required for the adoption
 91 of opinions, behavioral patterns, products, etc. Such a process is enhanced by communities, in which
 92 individuals are repeatedly exposed to the same ideas. This contrasts with *simple contagion* (modeled, for
 93 example, by independent cascades), in which similarly to disease spreading, only one contact is required to
 94 spread a message. An immediate consequence of such different dynamics is that hubs typically represent
 95 the best influencer under a simple contagion dynamics, whereas targeting low-degree nodes may yield a
 96 larger spread for complex contagion (Alshamsi et al., 2017). By including predispositions to resist change
 97 in our model nodes can spontaneously revert to the uninfluenced state. Therefore, the proposed model
 98 reflects the repeated exposure needed in complex contagion to influence a node with high probability.
 99 Alshamsi et al. (Alshamsi et al., 2017) has recently shown that it may be best to influence low-degree
 100 nodes in complex contagion in a setting in which nodes are committed to a state once adopted. Our results
 101 complement these findings in dynamic settings and show further conditions under which it is best to target
 102 low-degree nodes instead of hub nodes.

103 Our study is organized as follows. In Section 2 we give a detailed description of the model employed and
 104 describe analytical and numerical methods to find optimal control strategies. Section 3 then gives our main
 105 findings and we finish with a summary and discussion in Section 4.

2 METHODS

106 In the following we consider a variant of the voter model (Holley and Liggett, 1975; Clifford and Sudbury,
 107 1973) that accounts for spontaneous changes of opinions with a probability q . Let there be N agents with
 108 binary states $s_i = 1$ or $s_i = 0$, $i = 1, \dots, N$ which are connected by an unweighted social network given
 109 by its adjacency matrix $A = (a_{ij})_{i,j=1}^N$. We consider undirected connections, hence $a_{ij} = a_{ji} = 1$ if there

110 is a link between i and j and $a_{ij} = a_{ji} = 0$ otherwise. Additionally, we consider an external controller
 111 with opinion $s = 1$ who aims to align the system to its opinion. Control is exerted through the presence
 112 of additional in-neighbors with $s = 1$, i.e. a controlled node has an enhanced likelihood of choosing a
 113 neighbor with state $s = 1$ when updating. The controller thus influences the system through unidirectional
 114 links given by a vector $\vec{p} = (p_1, \dots, p_N)$ where $p_i = 1$ if the controller influences node i and $p_i = 0$
 115 otherwise. Without loss of generality we assume that $s = 1$ is the desired state into which the controller
 116 wants to guide the system. However, ‘convinced’ agents in state $s = 1$ may spontaneously revert to state
 117 $s = 0$.

118 In more detail, after random initialization of voters the dynamics of opinions are updated as follows:
 119 (i) a focus agent x is picked at random, (ii) with probability $(1 - q)$ agent x randomly selects one of its
 120 in-neighbors y and adopts the opinion of y , i.e., $s_x = s_y$. In the opposite case, i.e., with probability q ,
 121 if in state $s = 1$ agent x will spontaneously revert to state $s = 0$. Steps (i) and (ii) are repeated until an
 122 equilibrium is reached.

123 The above process allows for analytical solutions. Define u_i as the probability that node i will be in state
 124 $s = 1$. We can then write down the master equation

$$\dot{u}_i = (1 - q)/\Sigma_i \left((1 - u_i) \left(\sum_j a_{ji} u_j + p_i \right) - u_i \sum_j a_{ji} (1 - u_j) \right) - qu_i, \quad (1)$$

125 where

$$\Sigma_i = \sum_j a_{ji} + p_i \quad (2)$$

126 is the in-strength or the sum of influences node i experiences. The first term in Eq. (1) captures the typical
 127 copying dynamics of the voter model which occurs with probability $1 - q$ (see, e.g. (Masuda, 2015)), and
 128 the second term $-qu_i$ accounts for spontaneous flips back into the uncontrolled state.

129 Equilibrium states can be obtained from

$$(\text{diag}(\Sigma_i) - (1 - q)A) \vec{u}^* = (1 - q)\vec{p}, \quad (3)$$

130 where $\vec{u}^* = (u_1^*, \dots, u_N^*)$ denotes the vector of equilibrium probabilities and $\text{diag}(\Sigma_i)$ stands for a diagonal
 131 matrix D with entries $D_{ii} = \Sigma_i$ (cf. appendix 4 for more detail). Again following (Masuda, 2015) we next
 132 note that Eq. (3) gives a linear system which is diagonally dominant for all q . Thus, an efficient way of
 133 solving system (4) is by Jacobi iteration, where we start with $u_i^{(0)} = 1/2$, $i = 1, \dots, N$ and then iterate

$$u_i^{(n+1)} = (1 - q)/\Sigma_i \left(p_i + \sum_j a_{ji} u_j^{(n)} \right), \quad (4)$$

134 where superscripts indicate the iteration number. Stationary solutions \vec{u}^* then allow to estimate the share of
 135 votes influenced by the controller via $X = 1/N \sum_i u_i^*$.

136 From Eq. (3) we can also read the mean-field solution for the controlled vote share when controllers are
 137 allocated randomly on an all-to-all connected network, finding

$$X = \frac{1 - q}{\rho + q} \rho, \quad (5)$$

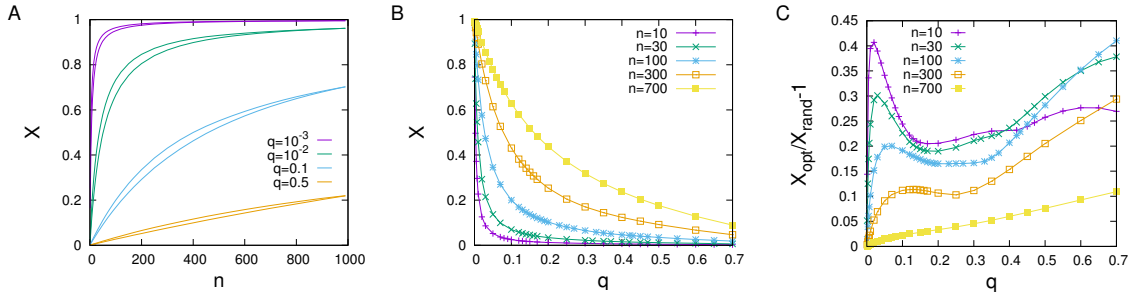


Figure 1. (A) Dependence of the controlled share of votes X on the resource of the controller n . For each color, the lower curve gives the vote share for random allocation of control and the upper curve vote shares for optimized allocations. (B) Dependence of optimized vote shares on the predisposition parameter q for various control resource endowments n . (C) Optimization gain relative to random control allocation for the scenario shown in (B). The data are for networks composed of $N = 1000$ nodes constructed for $\alpha = 3$ and each data point represents an average over 50 randomly sampled network configurations. Error bars are of the size of the lines/points.

138 where $\rho = 1/N \sum_i p_i$ is the density of controlled voters. It is straightforward to see the limiting cases of
 139 $q = 0$ and $q = 1$ in Eq. (5) corresponding to a perfectly controlled system ($X = 1$) and an uncontrollable
 140 system ($X = 0$), respectively. We can thus see that predisposition to resist change in the form of the
 141 flipping probability q quantify how difficult it is to control the system.

142 In the following we are interested in optimal control strategies (as quantified by \vec{p}) for the external
 143 controller for given networks. As a model for social networks we construct networks with power-law
 144 degree distributions $P(k) \propto k^{-\alpha}$ according to the configuration model (Newman, 2010). For given control
 145 resource $n = \sum_i p_i$ controls \vec{p} are then first assigned randomly and then optimized using a stochastic
 146 hill climber. More precisely, we iterate the following scheme: (i) select a controlled node x and a yet
 147 uncontrolled node y at random, (ii) rewire the control from x (i.e., $p_x = 1, p_y = 0$) to y (i.e., $p_x = 0,$
 148 $p_y = 1$) if $X(p_x = 1, p_y = 0) \leq X(p_x = 0, p_y = 1)$. Optimization using steps (i) and (ii) is stopped once
 149 no rewiring of controls has been accepted for a certain number T of attempts and three different initial
 150 control allocations are explored to reduce the probability of ending up in local optima with stochastic
 151 hill-climbing. For network sizes of $N = 1000$ nodes/voters that we shall investigate below, we typically
 152 set $T = 10^4$, which makes sure no substantial improvements in control can be found any more. If not
 153 mentioned otherwise, we set $\alpha = 3$ and run experiments with connectivity $\langle k \rangle = 3$. In the following, we
 154 will explore the dependence of optimal opinion control strategies on the predisposition parameter q for
 155 various resource allocations n to the controller.

3 RESULTS

156 In this section we present our main findings. We start by outlining numerical results in subsection 3.1 and
 157 then analyze two toy models, i.e. star networks and chains in subsection 3.2. Exact solutions for the toy
 158 models illustrate the main claim of the paper and give analytical insight into the shift from optimal high- to
 159 low-degree control.

160 3.1 Numerical Results

161 In Figure 1 simulation results on optimal vote control for scale-free networks of size $N = 1000$
 162 constructed for a scaling exponent $\alpha = 3$ are visualized. Panel 1A compares the dependence of optimal vote
 163 shares and average vote shares under random allocation of control on the controller's resource endowment

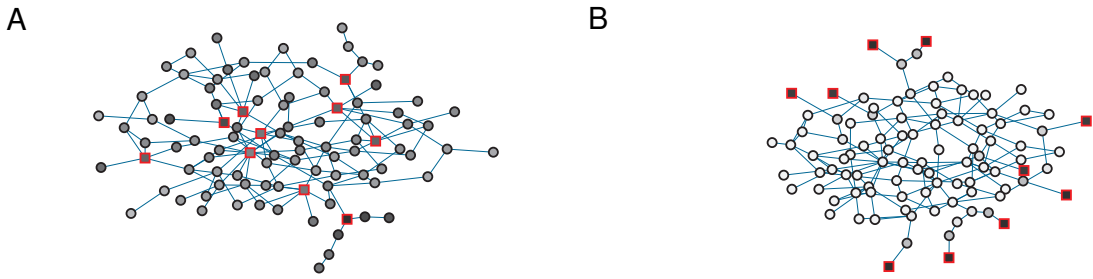


Figure 2. Examples of optimized control for a network of $N = 100$ nodes and $L = 288$ links for low $q = 0.01$ (left) and high $q = 0.5$ (right). The networks are constructed via a configuration model with $P(k) \propto k^{-\alpha}$ with $\alpha = 3$. Red boxes indicate controlled nodes, circles indicate ordinary nodes. Interior colors give relative control on a sliding scale from white (weakest control) to black (strongest control). The average opinion is $\langle s \rangle = 0.72$ (left) and $\langle s \rangle = 0.034$ (right).

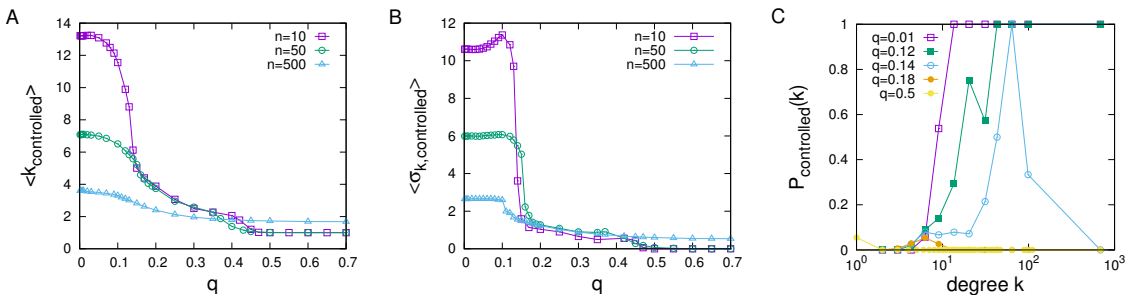


Figure 3. Dependence of optimal strategies for opinion control on the predisposition parameter q : (A) average degree of controlled nodes, (B) degree variance of controlled nodes. (C) Dependence of the probability of a node to be controlled on degree for control optimized for different values of q for $n = 10$. The data are for networks of $N = 1000$ nodes with $\alpha = 3$ and $\langle k \rangle = 3$ and in (A) and (B) each data point represents an average over 50 samples.

164 n for various predisposition strengths q . As one would expect, the larger the resource endowment n and
 165 the lower q , the larger the share of controlled votes. Panel Fig. 1B gives a further illustration of related
 166 experiments in which the optimal controller's resource endowment was fixed, but the magnitude of q
 167 systematically varied. We again see that larger resource levels allow for tighter control, but the effects of
 168 control decline strongly with q . One notes that optimal placement of control can considerably improve vote
 169 shares relative to random allocation (cf. Fig. 1C), but absolute improvements due to optimization are very
 170 limited when either q or n are large. Maximum gains achievable by optimization starting from random
 171 allocations tend to be around 40 – 50% of the initial vote share.

172 What are the best resource allocations? We proceed by investigating the dependence of optimal control
 173 strategies on the strength of predispositions q . Figure 2 gives an illustration of some first results for a
 174 small network of $N = 100$ nodes where control was evolved for situations of low (left) and high (right)
 175 predisposition strength for a controller which can influence 10 nodes. In the figure, controlled nodes are
 176 indicated by red boxes and the shading of nodes gives their average opinion state u for the chosen control
 177 scheme. Prevailing dark colors of nodes make it immediately obvious that the network can be strongly
 178 influenced in the low predisposition regime visualized in Fig. 2A but largely resists control in the high
 179 predisposition regime in Fig. 2B in which light colors dominate.

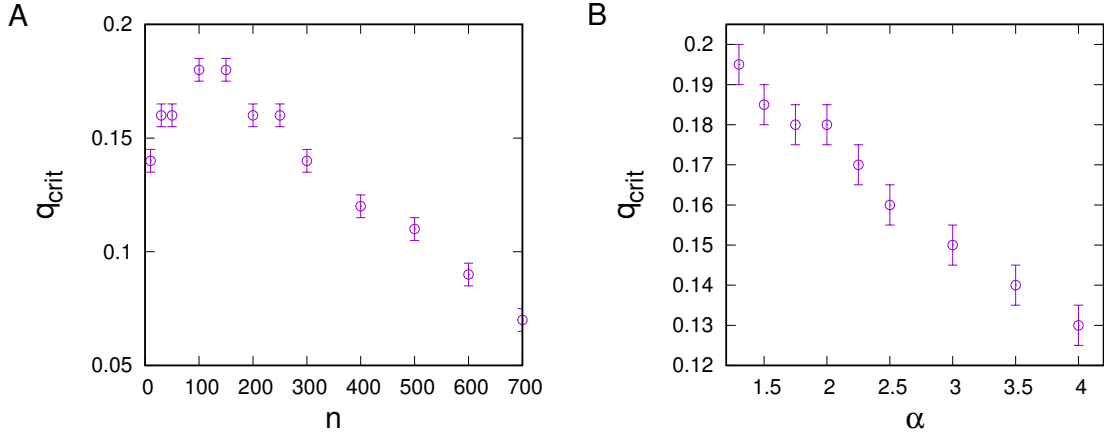


Figure 4. Dependence of the critical predisposition strength at which optimal control switches from hub control to low-degree control on (A) the total resource endowment of the controller n , (B) network heterogeneity for resource endowment $n = 10$ for the controller. The data are for networks of $N = 1000$ with connectivity $\langle k \rangle = 3$ and error bars result from the discretization of q -values when constructing $\sigma_{k,\text{controlled}}(q)$ plots.

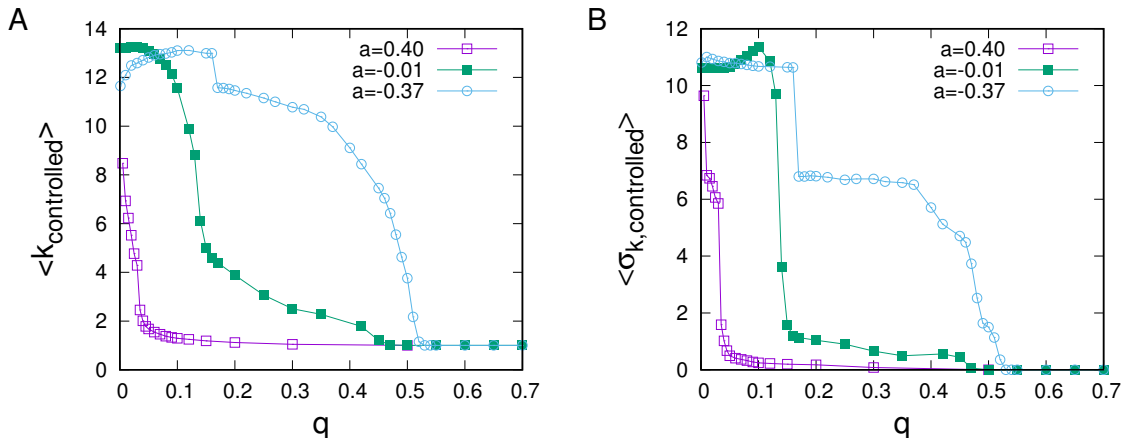


Figure 5. Dependence of average controlled degree (A) and standard deviation of controlled degrees (B) on the predisposition to resist for social networks of different assortativity. The data are for networks of $N = 1000$ nodes with $\alpha = 3$ and $\langle k \rangle = 3$ and data points represents averages over 50 runs.

180 For a more systematic investigation, we define the average degree of a controlled node

$$k_{\text{controlled}} = \frac{\sum_i p_i k_i}{\sum_i p_i}, \quad (6)$$

181 where $k_i = \sum_j a_{ij}$ is the degree of node i . Similarly, we also measure the standard deviation

$$\sigma_{k,\text{controlled}}^2 = \frac{\sum_i p_i (k_i - k_{\text{controlled}})^2}{\sum_i p_i}. \quad (7)$$

182 of the distribution of controlled node degrees. To gain further insights about the dependence of control on
183 degree we also estimate likelihoods $P_{k,\text{controlled}}$ of nodes to be controlled depending on their degrees.

184 The dependence of all three measures on q are plotted in Fig. 3A,B,C for various resource endowments n .
185 As also seen in the example above, the figure suggests the existence of two control regimes. For small q
186 control is clearly focused on the highest degree nodes. The smaller n the larger the average degree of the
187 n highest degree nodes, and accordingly we see relatively lower average degrees of controlled nodes the
188 larger n . In contrast, for large q control is clearly focused on low-degree nodes. In fact, as we see in the plot
189 of the dependence of standard deviations of degrees of controlled nodes vs. the strengths of predispositions
190 q , there is a sharp transition between the two control regimes, cf. Fig. 3B. Starting from low q up to some
191 critical point in q , the largest degree nodes are controlled in every instance, but control gradually includes
192 more and more low-degree nodes (see Fig. 3C). Beyond this point, control suddenly excludes the largest
193 degree nodes and focuses on a mixture of low-degree nodes before eventually becoming firmly fixed on
194 low-degree nodes for large q .

195 The low-high standard deviation regime threshold depends on resource endowments. To evaluate this
196 dependence we have measured q -dependencies of $\langle \sigma_{k, \text{controlled}} \rangle$ for various resource endowments n and
197 determined critical points from the sharp transitions in the respective $\langle \sigma_{k, \text{controlled}} \rangle(q)$ plots. Results are
198 illustrated in Fig. 4A, where we see that thresholds between the regimes initially grow with n , then saturate,
199 and decline.

200 We also investigated dependencies of thresholds on the structure of the social network to be controlled
201 as quantified by the degree exponent α . For this purpose, we constructed configuration type models with
202 fixed numbers of links for a range of α -parameters and again estimated critical points from the respective
203 $\langle \sigma_{k, \text{controlled}} \rangle(q)$ plots. Results are shown in Fig. 4B, where we see that more degree heterogeneous networks
204 generally support a larger high-degree control regime.

205 All of the experiments conducted above have been carried out for networks with given degree
206 heterogeneity, but without higher order correlations such as clustering or assortativity which are typical
207 for real-world networks (Newman, 2010). Because of the observed strong dependence of optimal control
208 on degree, the impact of degree-mixing patterns on the optimal control allocation appears of particular
209 interest. To address this question, we have constructed synthetic scale-free networks with dis-assortative
210 and assortative degree mixing patterns. Such networks can be generated by starting from a neutrally
211 assortative network and then randomly picking two connected pairs of nodes, ordering the nodes by degree,
212 and rewiring to change connections towards linking the pair of nodes with highest and the pair with lowest
213 degree (for increased assortativity) or re-linking nodes with largest degree differences (for dis-assortative
214 mixing). Rewiring according to this scheme preserves the overall degree sequence and allows to tune
215 degree mixing (Xulvi-Brunet and Sokolov, 2005). To investigate the role of degree mixing on control
216 schemes, we have carried out rewiring to tune assortativity until no further reconnection moves could
217 be carried out, resulting in networks with very strong dis-assortative and assortative degree mixing with
218 $a = -0.37$ and $a = 0.40$ measured by Newman's assortativity coefficient (Newman, 2003). Results for
219 optimal control allocations for such networks are shown in Fig. 5. It becomes apparent that assortativity
220 has a strong influence on optimal control: Whereas the regime of hub control is strongly reduced for
221 assortative networks it is considerably extended for the case of dis-assortative degree mixing. As we shall
222 see below, for $q > 0$ nodes are the more difficult to control, the larger their degree. Thus, in an assortatively
223 mixed network, hub nodes tend to be surrounded by nodes which are difficult to control, making it even
224 more difficult to control the hub node itself. The effect results in a much lowered threshold for q at which
225 periphery control becomes optimal. The contrary argument applies for disassortative networks. In this case
226 hub nodes are surrounded by nodes that can be more easily controlled, which, in turn, makes them easier to
227 control even at large q , resulting in an extension of the regime of optimal hub control.

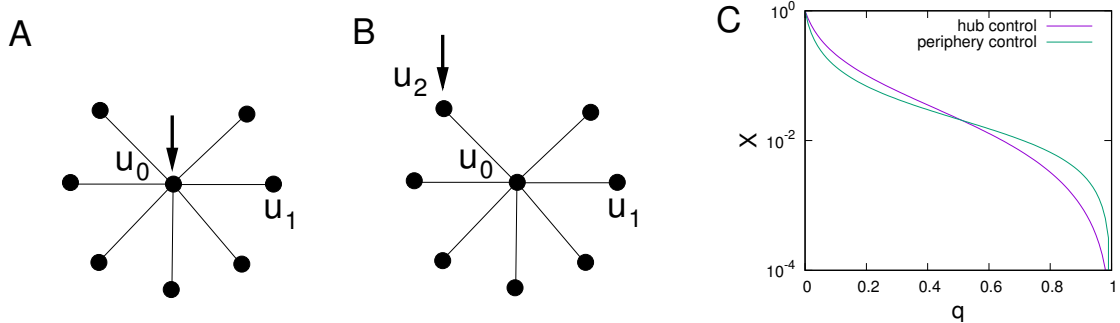


Figure 6. Illustration of a star network with control targeted at a central hub (A) and control targeted at a periphery node (B) and dependence of the average stationary vote shares for both scenarios on q (C) for a star network with one central hub and $k = 15$ spokes. Average probabilities of being in the controlled state are labeled u_0 for the hub node, u_1 for uncontrolled periphery nodes, and u_2 for a controlled periphery node.

228 3.2 A Model of Star Networks and Chains

229 To understand changes in optimal control strategies depending on predisposition strengths we give an
 230 analytical argument for a star network and analyze two control scenarios: control of strength one focused
 231 at the central hub and control of strength one focused on a single peripheral node, cf. Fig. 6A and Fig.
 232 6B, respectively. Note that Masuda (2015) has also analyzed this toy network for the original voter model
 233 with a passive controller, finding that single node control should always be focused on the central hub in
 234 that case. As an illustrative example to investigate how the effects of control change with distance from a
 235 directly controlled node, we also investigate control of an undirected chain by placing a controller at one of
 236 the ends of the chain.

237 Our arguments below are based on applying Eq. (3) to the star network. With some algebraic manipulation
 238 (see Appendix 4 for a detailed derivation) for control of strengths $p_0 = 1$ applied to the central hub, we
 239 obtain $u_0 = (1 - q)/(1 + kq(2 - q))$ and $u_1 = (1 - q)u_0$ and thus

$$X_{\text{central}} = \frac{k(1 - q) + 1}{k + 1} \frac{1 - q}{1 + kq(2 - q)}, \quad (8)$$

240 where k is the number of spoke nodes. For the periphery controlled scenario similar calculations yield
 241 $u_1 = (1 - p)u_0$, $u_0 = (1 - q)/(k - (1 - q)^2(k - 1))u_2$ and $u_2 = (1 - q)/(2 - (1 - q)^2/(k - (1 - q)^2(k - 1)))$
 242 resulting in

$$X_{\text{periphery}} = \frac{f + (1 - q)(k - 1)f + 1}{k + 1} \frac{1 - q}{2 - (1 - q)f}, \quad (9)$$

243 where

$$f = \frac{1 - q}{(1 - q)^2 + kq(2 - q)}. \quad (10)$$

244 Comparison of $X_{\text{central}}(q)$ with $X_{\text{periphery}}(q)$ reveals changes in the optimal strategy when q is increased,
 245 cf. Fig. 6C where we illustrate this scenario for $k = 15$ and observe that for low q hub control is
 246 optimal whereas for large q periphery control proves superior. To analyze what control strategy performs
 247 better depending on q we first note that $X_{\text{central}}(q = 0) = X_{\text{periphery}}(q = 0) = 1$ and observe that
 248 $\partial X_{\text{periphery}}/\partial q|_{q=0} = (1 - 2k - 4k^2)/(k + 1)$ whereas $\partial X_{\text{central}}/\partial q|_{q=0} = (-1 - 4k - 2k^2)/(k + 1)$, i.e.,
 249 for $k \geq 2$ after starting at the same point for $q = 0$ the effectiveness of central control initially decays

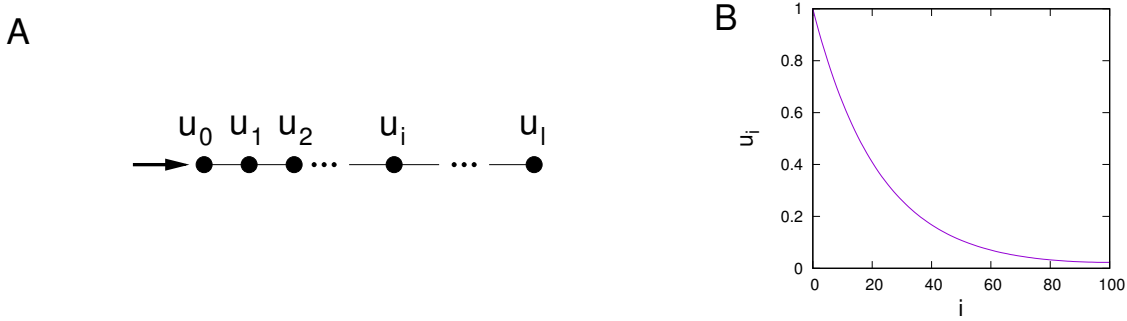


Figure 7. Illustration of a chain network with control targeted at node 0 at the left end (A) and dependence of the average stationary vote shares u_i depending on the distance i to the directly controlled node (B) for a chain of length 100 and $q = 0.01$ calculated based on Eq. (19).

250 slower with q than the effectiveness of peripheral control. Thus, for small q one has $X_{\text{central}} > X_{\text{periphery}}$.
 251 As for both control scenarios $X_{\text{central}}(q = 1) = X_{\text{periphery}}(q = 1) = 0$, similar analysis of slopes at $q = 1$
 252 shows that $X_{\text{central}} < X_{\text{periphery}}$ for q close to 1.

253 Instead of a not very instructive exact calculation of the critical point q_{crit} at which optimal control
 254 switches, we limit the analysis to the case of large k . Figure 6C suggests that $q_{\text{crit}} \approx 1/2$ for large
 255 $k > 10$ in star networks. In fact, expansion of Eq.'s. (8) and (9) in leading order in $1/k$ confirms that
 256 $X_{\text{central}} > X_{\text{periphery}}$ for $q < 1/2$ and $X_{\text{central}} < X_{\text{periphery}}$ for $q > 1/2$ in the limit of $k \rightarrow \infty$.

More importantly, calculations in this toy model illustrate why hub control weakens at large values of q . We note that for any $q > 0$ nodes are the more difficult to control the larger their degree. In fact, whilst this effect vanishes for $q = 0$ hub control also becomes the more difficult, the larger q . However, nodes are also the more difficult to (indirectly) control the farther away they are in terms of network distance from the node directly influenced by the controller. To analyze the latter effect, consider a linear chain of length l , controlled by influence of strength one applied to either end, cf. Fig. 7A. Equation (3) applied to this situation then reads

$$2u_0 - (1 - q)u_1 = (1 - q) \quad (11)$$

$$\dots \quad (12)$$

$$2u_i - (1 - q)u_{i-1} - (1 - q)u_{i+1} = 0 \quad \dots \quad (13)$$

$$u_l - (1 - q)u_{l-1} = 0.$$

257 To solve the above system of linear homogeneous difference equations we use the ansatz $u_i = A\lambda^i$ for
 258 $i = 1, \dots, n - 1$ and find eigenvalues

$$\lambda_{1/2} = \frac{1}{1 - q} (1 \pm g), \quad (14)$$

with $g = \sqrt{q(2-q)}$. General solutions are thus of the form $u_i = A\lambda_1^i + B\lambda_2^i$. Matching with the boundary conditions for $i = 0$ and $i = 1$ gives two conditions to fix the values of the constants A and B

$$2(A + B) - (1 - q)(A\lambda_1 + B\lambda_2) = 1 - q \quad (15)$$

$$A(\lambda_1^l + B\lambda_2^l) - (1 - q)(A\lambda_1^{l-1} + B\lambda_2^{l-1}) = 0. \quad (16)$$

Solving for A and B one obtains

$$A = -B \frac{\lambda_2^{l-1} g - 1}{\lambda_1^{l-1} g + 1} \quad (17)$$

and

$$B = \frac{1 - q}{1 + \left(\frac{1-g}{1+g}\right)^{l+1}}. \quad (18)$$

We finally obtain

$$u_i = \frac{1}{(1 - q)^{i-1}} \frac{1}{1 + \left(\frac{1-g}{1+g}\right)^{l+1}} \left(\frac{(1-g)^l}{(1+g)^l} (1+g)^i + (1-g)^i \right). \quad (19)$$

259 We observe that for $i < l$ the second term in Eq. (19) is always substantially larger than the first. Noting
 260 also that $q < g(q)$ for $q \in (0, 1)$ it follows that u_i is decreasing with i , i.e. the example of the controlled
 261 chain network demonstrates that influence of indirect control on a node decreases with the distance from
 262 that node, cf. also Fig. 7B.

263 We thus see two opposing effects of hub control. On the one hand hubs are the more difficult to control the
 264 larger their degree. On the other hand, because a hub node has more neighbors than an average node, control
 265 of hub nodes provides a controller with closer access to other nodes in the network and this improved access
 266 can outweigh the enhanced difficulty of controlling high degree nodes for low predisposition strengths. In
 267 contrast, in high q settings the decreased controllability of hub nodes outweighs the enhanced access to the
 268 their respective neighbors that they provide to the controller.

4 DISCUSSION

269 In this paper we have investigated the impact of predispositions to return to the uninfluenced state on
 270 opinion control in a variant of the voter model. Results have shown that predisposition strength has
 271 a strong influence on optimal control strategies, such that essentially two control regimes exist. For
 272 low predisposition strength, optimal control is found to be focused on hub nodes, whereas for large
 273 predisposition strength optimal control should be focused on low-degree nodes. In the latter situation,
 274 controllers can only gain relatively little total influence over the system, but strategic allocation can still
 275 result in improvements of control gains of up to 40% relative to random allocation.

276 Through numerical simulations of the voting dynamics on scale-free networks and analytical calculations
 277 on star networks we have established that both regimes tend to be separated by a transition, with details
 278 of the transition depending on resource endowments of the controller and the heterogeneity of the social
 279 network. Our numerical results suggest that more heterogeneous networks (i.e., scale-free networks with

280 a smaller scaling exponent α) support a larger regime of optimal hub control than more homogeneous
281 networks.

282 Our main finding, i.e., the existence of regimes in which optimal control strategies should focus on
283 low-degree nodes, differs markedly from previous investigations of the original voter model (Yildiz et al.,
284 2013; Kuhlman et al., 2013; Masuda, 2015). A point that may serve to illustrate the reduced effectiveness
285 of hub control in the present model is that the model can be mapped to the conventional voter model with a
286 passive opponent who influences every voter on the social network. To account for the spontaneous state
287 reversion which occurs with constant probability for each node, in the mapped version of the standard voter
288 model such a passive controller would have to have control strengths to nodes proportional to their degree,
289 i.e., exert a much stronger influence on hub nodes than low-degree nodes (see Appendix 4 for details).
290 Thus, it is not surprising that a binary active controller may wish to focus on low-degree nodes. In this light
291 one might wonder why hub control is optimal for any value of q . As our toy example of a chain network
292 has illustrated, indirectly controlling nodes that do not have a direct connection from the controller comes
293 at a cost that grows with distance from the closest directly controlled node. Thus, hub nodes can still be
294 optimal because of their central topological position in the network such that average distances from them
295 to other nodes are lower than for low-degree nodes, potentially outweighing the enhanced difficulty in
296 gaining control over them.

297 In the presented model we have analyzed the case of binary scenarios in which nodes can either be
298 controlled or not, but controllers cannot choose the strengths of control. An alternative scenario could be an
299 allocation scheme in which controllers can distribute resource in such a way that some nodes are strongly
300 influenced and others only experience a weak effect. It is thus possible that our choice of binary control
301 could have affected the results. One could imagine that even in the low degree regime in the binary model
302 optimal continuous schemes that allocate very strong control to hubs could outperform evenly balanced
303 control that aims to influence many low-degree nodes. Investigations of the continuous scenario represent
304 an interesting avenue for future work.

305 Another point worth emphasizing is that we have considered undirected networks in this study. Results
306 in the voter dynamics may differ markedly on directed networks (Masuda, 2015). Moreover, on directed
307 networks in- and out-degrees of nodes might be uncorrelated such that out-degree hubs are not necessarily
308 in-degree hubs and vice versa. Difficulties in hub-control as described above relate to the difficulty of
309 node control with growing in-degree, whereas benefits of node control result from large out-degrees. One
310 can thus expect a more nuanced picture for directed networks in the presence of a predisposition to resist,
311 which should be worth studying in more detail in the future.

312 On a more speculative note, we remark that predispositions to return to the uninfluenced state in the
313 present model essentially introduce a degree-dependent resistance of nodes to align with the external
314 control. A rewrite of Eq. (1) shows that a very similar equation and essentially similar effects can be
315 observed when not introducing q a probability to return to the opposed state when in the influenced state,
316 but as a probability to flip state in *any* state. The latter phenomenon corresponds to noise, and it will be of
317 interest to carry out a more detailed comparison of results for the voting dynamics in this situation with the
318 results of Lynn and Lee (2016) for the kinetic Ising model.

APPENDIX A

319 Here we provide a more detailed derivation of Eq. (3). We start from Eq. (1), setting $u_i = 0$ to obtain a
320 stationarity condition. One notes that the quadratic terms proportional to products $u_i u_j$ cancel out and after

321 multiplication by Σ_i we find

$$0 = (1 - q) \left(\sum_j a_{ji} u_j + (1 - u_i) p_i - u_i \sum_j a_{ji} \right) - q \Sigma_i u_i. \quad (20)$$

322 Re-arranging terms and recalling $\Sigma_i = \sum_j a_{ji} + p_i$ yields

$$-(1 - q)p_i = (1 - q) \sum_j a_{ji} u_j - (1 - q)u_i p_i - (1 - q)u_i \sum_j a_{ji} - qu_i \sum_j a_{ji} - qp_i u_i \quad (21)$$

323 and thus

$$(1 - q)p_i = u_i \Sigma_i - (1 - q) \sum_j a_{ji} u_j, \quad (22)$$

324 which is Eq. (3).

APPENDIX B

325 In this section we provide some additional detail for the calculation of equilibrium shares for star
 326 networks with central and peripheral control (cf. section 3.2 and Fig. 6 for a pictorial representation
 327 of the corresponding networks). We start by analyzing central control, for which Eq. (3) reads

$$(k + 1)u_0 - (1 - q)ku_1 = (1 - q) \quad (23)$$

$$u_1 - (1 - q)u_0 = 0. \quad (24)$$

From (24) we find $u_1 = (1 - q)u_0$ and inserting into (23) yields

$$u_0((k + 1) - k(1 - q)^2) = (1 - q). \quad (25)$$

We thus find the expression for u_0 given in section 3.2. We further have

$$X_{\text{central}} = \frac{1}{k + 1}(u_0 + ku_1) \quad (26)$$

$$= \frac{u_0(1 + k(1 - q))}{k + 1}, \quad (27)$$

328 which results in Eq. (8) in section 3.2 after inserting u_0 .

We proceed with details of the calculation to obtain the controlled vote share for a periphery-controlled star. In this case, Eq. (3) reads:

$$ku_0 - (1 - q)(k - 1)u_1 - (1 - q)u_2 = 0 \quad (28)$$

$$u_1 - (1 - q)u_0 = 0 \quad (29)$$

$$2u_2 - (1 - q)u_0 = 1 - q. \quad (30)$$

329 We immediately see $u_1 = (1 - q)u_0$. Inserting into (28) and solving for u_2 gives the expression in section
 330 3.2 for u_2 which can be written in more convenient form using (10)

$$u_2 = \frac{1 - q}{2 - (1 - q)f}. \quad (31)$$

331 Finally, we have

$$X_{\text{periphery}} = \frac{1}{k + 1} (u_2 + fu_2 + (k - 1)(1 - q)fu_2), \quad (32)$$

332 which, after inserting u_2 , results in expression (9) in section 3.2.

APPENDIX C

333 In this section we provide a more detailed argument how the voting model with predisposition can be
 334 mapped to the original voter model in the presence of two opposing zealots, where the passive zealot has
 335 a control strength which is proportional to a node's degree. In the following, we shall label the active
 336 controller as A and its control influence as p_i^A (as opposed to just labeling its control gain by p_i in the rest
 337 of the paper), and label the passive controller as B with control gain p_i^B . We shall show that our Eq. (1) is
 338 equivalent to Eq. (3) in Masuda (2015) provided that the strength of the passive controller is proportional
 339 to the influence exerted on an agent by the social network and the active control, i.e. $p_i^B = \gamma(\sum_j a_{ji} + p_i^A)$.
 340 We first note that we can scale time in our Eq. (1) to obtain an equivalent condition

$$\dot{u}_i = (1 - q)/\sum_i \left((1 - u_i)(\sum_j a_{ji}u_j + p_i) - u_i \sum_j a_{ji}(1 - u_j) \right) - q/(1 - q)u_i, \quad (33)$$

341 We can now rewrite Eq. (33) as

$$\dot{u}_i = \frac{\sum_j a_{ij} + p_i^A + p_i^B}{\sum_j a_{ji} + p_i^A} \left((1 - u_i) \frac{\sum_j a_{ji}u_j + p_i}{\sum_j a_{ji} + p_i^A + p_i^B} - u_i \frac{\sum_j a_{ji}(1 - u_j)}{\sum_j a_{ji} + p_i^A + p_i^B} \right) - \frac{q}{1 - q} \frac{\sum_j a_{ij} + p_i^A + p_i^B}{\sum_j a_{ij} + p_i^A + p_i^B} u_i, \quad (34)$$

342 and thus

$$\dot{u}_i = (1 + \gamma) \left((1 - u_i) \frac{\sum_j a_{ji}u_j + p_i}{\sum_j a_{ji} + p_i^A + p_i^B} - u_i \frac{\sum_j a_{ji}(1 - u_j)}{\sum_j a_{ji} + p_i^A + p_i^B} \right) - \frac{q(1 + \gamma)}{(1 - q)\gamma} \frac{p_i^B}{\sum_j a_{ij} + p_i^A + p_i^B} u_i, \quad (35)$$

343 Again rescaling time by a factor $(1 + \gamma)$ we find

$$\dot{u}_i = \left((1 - u_i) \frac{\sum_j a_{ji}u_j + p_i}{\sum_j a_{ji} + p_i^A + p_i^B} - u_i \frac{\sum_j a_{ji}(1 - u_j) + q/(\gamma(1 - q))p_i^B}{\sum_j a_{ji} + p_i^A + p_i^B} \right), \quad (36)$$

344 which corresponds to Masuda's Eq. (3) provided we choose $\gamma = q/(1 - q)$. We thus see that the model
 345 with predisposition of strength q to resist influence is formally equivalent to the original controlled
 346 voter model with a passive controller who exerts a given degree-dependent control of strength $p_i^B =$
 347 $q/(1 - q)(\sum_j a_{ji} + p_i^A)$ on all nodes. As we consider binary control with $p_i^A \in \{0, 1\}$, p_i^B would have to
 348 be essentially proportional to degree for large degrees.

CONFLICT OF INTEREST STATEMENT

349 The authors declare that the research was conducted in the absence of any commercial or financial
350 relationships that could be construed as a potential conflict of interest.

AUTHOR CONTRIBUTIONS

351 M.B. designed the study, conducted and evaluated the experiments and wrote the paper. All authors
352 contributed to manuscript revision, read and approved the submitted version.

ACKNOWLEDGMENTS

353 The authors acknowledge the use of the IRIDIS High Performance Computing Facility, and associated
354 support services at the University of Southampton, in the completion of this work. This research was
355 sponsored by the U.S. Army Research Laboratory and the U.K. Ministry of Defence under Agreement
356 Number W911NF-16-3-0001. The views and conclusions contained in this document are those of the
357 authors and should not be interpreted as representing the official policies, either expressed or implied,
358 of the U.S. Army Research Laboratory, the U.S. Government, the U.K. Ministry of Defence or the U.K.
359 Government. The U.S. and U.K. Governments are authorized to reproduce and distribute reprints for
360 Government purposes notwithstanding any copyright notation hereon.

REFERENCES

361 Albert, R. and Barabási, A.-L. (2002). Statistical mechanics of complex networks. *Rev. Mod. Phys.* 74,
362 47–97

363 Alshamsi, A., Pinheiro, F., and Hidalgo, C. (2017). When to target hubs? strategic diffusion in complex
364 networks. *arXiv:1705.00232v1*

365 Arendt, D. L. and Blaha, L. M. (2015). Opinions, influence, and zealotry: a computational study on
366 stubbornness. *Comput. Math. Organ. Theory* 21, 184–209

367 Bharathi, S., Kempe, D., and Salek, M. (2007). Competitive influence maximization in social networks.
368 *Internet and Network Economics, Lect. Notes Comput. Sci.* 4858, 306–311

369 Bharathi, S., Kempe, D., and Salek, M. (2010). Threshold models for competitive influence in social
370 networks. *Proc. Workshop on Internet and Network Economics, WINE (2010)* 4858, 539–550

371 Castellano, C., Fortunato, S., and Loreto, V. (2009). Statistical physics of social dynamics. *Rev. Mod. Phys.*
372 81, 591–646

373 Centola, D. (2010). The spread of behavior in an online social network experiment. *Science* 329,
374 1194–1197

375 Centola, D., Eguíluz, V. M., and Macy, M. W. (2007). Cascade dynamics of complex propagation. *Physica*
376 A 374, 449–456

377 Centola, D. and Macy, M. (2007). Complex contagions and the weakness of long ties. *Am. J. Sociol.* 113,
378 702–734

379 Clifford, P. and Sudbury, A. (1973). A model for spatial conflict. *Biometrika* 60, 581–588

380 Easley, D. and Kleinberg, J. (2010). *Networks, Crowds and Markets: Reasoning About a Highly Connected*
381 *World* (Cambridge University Press, New York, NY, 2010.)

382 Goyal, S., Heidari, H., and Kearns, M. (2014). Competitive contagion in networks. *Games and Economic*
383 *Behaviour* doi:<https://doi.org/10.1016/j.geb.2014.09.002>

384 Hegselmann, R., König, S., Kurz, S., Niemann, C., and Rambau, J. (2015). Optimal opinion control: The
385 campaign problem. *Journal of Artificial Societies and Social Simulation* 18

386 Hill, A. L., Rand, D. G., Nowak, M. A., and Christakis, N. A. (2010). Infectious disease modeling of social
387 contagion in networks. *PLoS Comput. Biol.* e1000968

388 Holley, R. and Liggett, T. (1975). Ergodic theorems for weakly interacting infinite systems and the voter
389 model. *Ann. Probab.* 3, 643–663

390 Hu, H. and Zhu, J. J. H. (2017). Social networks, mass media and public opinions. *J. Econ. Interact. Coord.*
391 12, 393–411

392 Kempe, D., Kleinberg, J., and Tardos, E. (2003). Maximizing the spread of influence through a social
393 network. *Proceedings of the Ninth International Conference on Knowledge discovery and Data Mining*
394 (KDD), Washington, DC, USA , 137–146

395 Khalil, N., San Miguel, M., and Toral, R. (2018). Zealots in the mean-field noisy voter model. *Phys. Rev.*
396 E 97, 012310

397 Kuhlman, C. J., Anil Kumar, V. S., and Ravi, S. S. (2013). Controlling opinion propagation in online
398 networks. *Computer Networks* 57, 2121–2132

399 Laciana, C. E. and Rovere, S. L. (2011). Ising-like agent-based technology diffusion model: Adoption
400 patterns vs. seeding strategies. *Physica A* 390, 1139–1149

401 Liu, S. and Shakkottai, S. (2010). Influence maximization in social networks: An ising-model-based
402 approach. *Proceedings of the Forty-Eighth Annual Allerton Conference* , 570–576

403 Lynn, C. W. and Lee, D. D. (2016). Maximizing influence in an ising network: A mean-field optimal
404 solution. *Proceedings of the 30th conference on neural information processing systems (NIPS 2016)* ,
405 1–9

406 Masuda, M., Gilbert, N., and Redner, S. (2010). Heterogeneous voter models. *Phys. Rev. E* 82, 010103

407 Masuda, M. and Redner, S. (2011). Can partisan voting lead to truth? *J. Stat. Mech.* , L02002

408 Masuda, N. (2015). Opinion control in complex networks. *New Journal of Physics* 17, 033031

409 Mobilia, M. (2003). Does a single zealot affect an infinite group of voters? *Phys. Rev. Lett.* 91, 028701

410 Mobilia, M. (2015). Nonlinear q-voter model with inflexible zealots. *Phys. Rev. E* 92, 012803

411 Mobilia, M. and Georgiev, I. T. (2005). Voting and catalytic processes with inhomogeneities. *Phys. Rev. E*
412 71, 046102

413 Mobilia, M., Petersen, A., and Redner, S. (2007). On the role of zealotry in the voter model. *J. Stat. Mech.*
414 , P08029

415 Morone, F. and Makse, H. A. (2015). Influence maximization in complex networks through optimal
416 percolation. *Nature* 524, 65–68

417 Newman, M. E. J. (2003). Mixing patterns in networks. *Phys. Rev. E* 67, 026126

418 Newman, M. E. J. (2010). *Networks: An introduction* (Oxford University Press)

419 Quax, R., Apolloni, A., and Sloot, P. M. (2013). The diminishing role of hubs in dynamical processes on
420 complex networks. *J. R. Soc. Interface* 10, 20130568

421 Romero, D. M., Meeder, B., and Kleinberg, J. (2011). Differences in the mechanics of information
422 diffusion across topics: Idioms, political hashtags, and complex contagion on twitter. *Proc. 20th Int.*
423 *Conf. on World Wide Web (ACM)*

424 Sirbu, A., Loreto, V., Servedio, V. P. D., and Tria, F. (2016). Opinion dynamics: Models, extensions and
425 external effects. *Participatory Sensing, Opinions and Collective Awareness* , 363–401

426 Waagen, A., Verma, G., Chan, K., Swami, A., and D’Souza, R. (2015). Effect of zealotry in high-
427 dimensional opinion dynamic models. *Phys. Rev. E* 91, 022811

428 Xulvi-Brunet, R. and Sokolov, I. M. (2005). Changing correlations in networks: assortativity and
429 disassortativity. *Acta Physica Polonica* 36, 1431–1455

430 Yildiz, E., Ozdaglar, A., Acemoglu, D., Saberi, A., and Scaglione, A. (2013). Binary opinion dynamics
431 with stubborn agents. *ACM Transactions on Economics and Computation* 1, 19